Journal of Applied Polymer Science

Inkjet printing of polyimide insulators for the 3D printing of dielectric materials for microelectronic applications

Fan Zhang, Christopher Tuck, Richard Hague, Yinfeng He, Ehab Saleh, You Li, Craig Sturgess, Ricky Wildman

Additive Manufacturing and 3D Printing Research Group, Faculty of Engineering, Nottingham University, Nottingham NG7 2RD, United Kingdom

Correspondence to: F. Zhang (E-mail: fan.zhang@nottingham.ac.uk)

ABSTRACT: In this article, we report the first continuous fabrication of inkjet-printed polyimide films, which were used as insulating layers for the production of capacitors. The polyimide ink was prepared from its precursor poly(amic) acid, and directly printed on to a hot substrate (at around 160 °C) to initialize a rapid thermal imidization. By carefully adjusting the substrate temperature, droplet spacing, droplet velocity, and other printing parameters, polyimide films with good surface morphologies were printed between two conducting layers to fabricate capacitors. In this work, the highest capacitance value, 2.82 ± 0.64 nF, was achieved by capacitors (10 mm × 10 mm) with polyimide insulating layers thinner than 1 μm, suggesting that the polyimide inkjet printing approach is an efficient way for producing dielectric components of microelectronic devices. © 2016 The Authors Journal of Applied Polymer Science Published by Wiley Periodicals, Inc. J. Appl. Polym. Sci. **2016**, *133*, 43361.

KEYWORDS: dielectric properties; manufacturing; polyimides; rheology

Received 13 October 2015; accepted 17 December 2015

DOI: 10.1002/app.43361

INTRODUCTION

Polyimides (PIs) are a class of polymers with excellent thermal stability, chemical resistance, mechanical and electrical properties.[1–3] Due to these outstanding properties, PIs have been considered to be suitable candidates for microelectronic applications, such as interlayer dielectrics[4] and protective layers in integrated circuit fabrication and MEMS devices.[5]

Polyimide can be prepared from its precursor poly(amic) acid (PAA) upon heating or chemical treatment,[1] which allows the use of spin coating to prepare PI thin films followed by lithography to fabricate MEMS parts.[6] However, conventional lithography methods require the use of photoresist as well as complicated processing steps (including soft bake, hard bake, developing of photoresist, etc.),[2,6] which make part fabrication a slow, costly, and an environmentally unfriendly process. Therefore, there is a need to bypass these fabrication steps and seek a more efficient way for high-precision PI fabrication.

In recent publications, PI films have been fabricated using inkjet printing (IJP) technology to act as the insulating layers in capacitors[7] and biosensors.[8] IJP can also be used as a potential additive manufacturing (AM) process, during which one drop of material is deposited at a time to build three dimensional structures.[9] IJP techniques are considered to be especially suitable for fabricating microelectronic devices due to their various advantages, such as simplicity of fabrication, compatibility with various substrates,[7] noncontact process and low cost.[11] Recently, there have been some advances in producing alternative metallic conducting inks that can be fabricated using IJP, such as the low temperature reactive silver ink reported by Walker and Lewis.[12] These advances, in tandem with being able to IJP PI insulating inks, offers IJP as a promising route to alternative fabrication methods for microelectronic devices.

Prior research has shown the use of printed PI layers in electronic devices[7,8] through a two-step method, during which PAA solutions were jetted followed by a thermal imidization process. However, no detailed printing procedures and product qualities, including morphology and electronic properties, were reported in their work. Determining the film quality is a high priority before applying PI insulating layers on microelectronics, especially for ultrathin layers, where tiny pinholes or surface waviness can result in reduced properties. In this

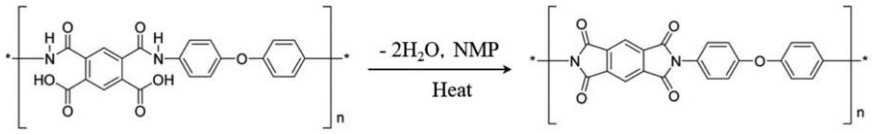

Figure 1. Thermal imidization process of forming PI from its precursor PAA.

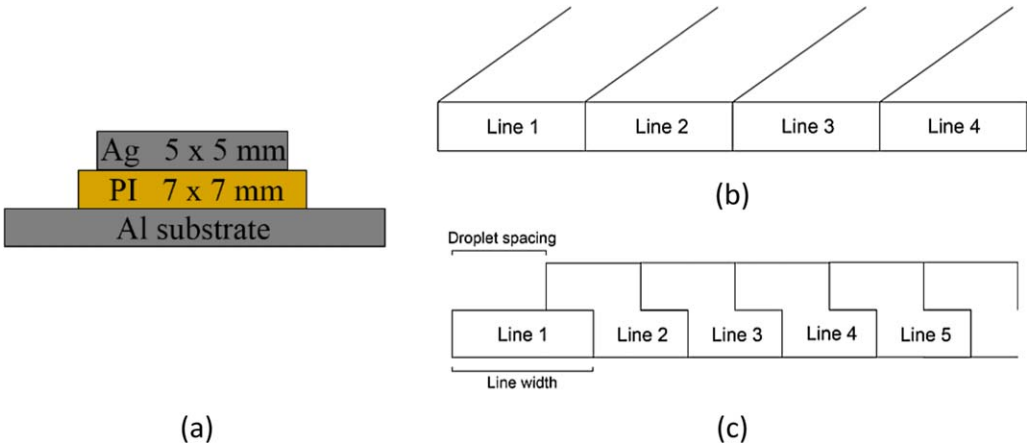

Figure 2. (a) A parallel plate capacitor structure formed by sandwiching PI layer with Ag layer and aluminum substrate; (b) a normal pattern; and (c) a pattern with 30% overlap between connecting lines. [Color figure can be viewed in the online issue, which is available at wileyonlinelibrary.com.]

article, a one-step IJP process to prepare a PI insulating layer is reported, including a comprehensive study of the printability of the inks, their required printing parameters and resultant film qualities.

METHODOLOGY

Ink Preparations

Poly(pyromellitic dianhydride-*co*−4,′-oxydianiline) amic acid (PAA) solution (12.8 wt % ± 0.5 wt % PAA in 80% 1-methyl-2-pyrrolidinone (NMP)/20% aromatic hydrocarbon, Sigma-Aldrich) was directly diluted using NMP (≥99.0%, Sigma-Aldrich) to make 1 wt %, 3 wt %, and 5 wt % solutions. The solutions were stirred at 800 rpm at room temperature for 10 min to improve the dispersion of PAA, followed by ultrasonication for 30 min to remove bubbles and to further disperse the PAA.

Printability Assessment

The printability of an ink can be estimated by the Z number,[13] which is defined as

$$Z = \frac{\sqrt{\rho r \gamma}}{\mu} \quad (1)$$

where ρ is the density (g cm^{-3}), r is the orifice diameter (μm), γ is the surface tension of the fluid (mN m^{-1}), and μ is the viscosity of the ink (mPa S). An ink can be considered to be printable when Z falls between 1 and 10.[14] The viscosity and surface tension of the PAA/NMP inks were measured to determine the Z number. The viscosity was assessed using a cone plate rheometer (Malvern Kinexus Pro) with a shear rate sweep between 10 and 1000 s^{-1} within a temperature range of 20 °C to 70 °C, while the surface tension and contact angle were measured at 20 °C using a Kruss DSA100S pendant drop shape analyser.

Thermal Imidization Conditions

After printing the PAA/NMP ink, a thermal imidization process was necessary to convert PAA to PI[4] (Figure 1). The imidization process was monitored using Fourier Transform-Infrared Red (FT-IR) spectroscopy, during which a Bruker Tensor 27 FT-IR with a Specac heated golden gate attenuated total reflectance (ATR)

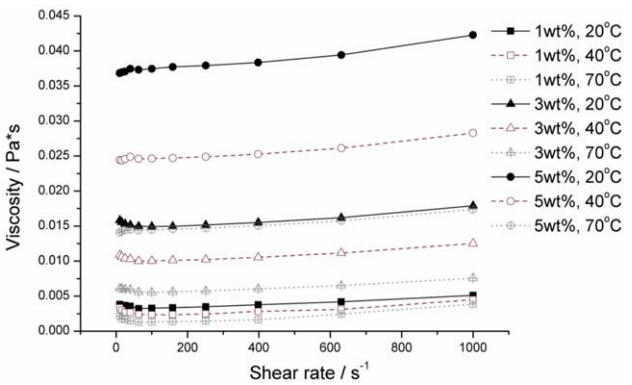

Figure 3. Viscosities of 1 wt %, 3 wt %, and 5 wt % PAA/NMP inks tested from 20 °C to 70 °C with shear rate range between 1 s^{-1} and 1000 s^{-1}. [Color figure can be viewed in the online issue, which is available at wileyonlinelibrary.com.]

Table I. Material Properties and Printability Index Z of the 1 wt % PAA/NMP Ink

Sample	Nozzle diameter (μm)	Density (g cm^{-3})	Viscosity (at 1000 s^{-1}) (mPa S)	Surface tension (mN m^{-1})	Z (Oh^{-1})
1 wt % ink	21	1.03	5.11	39.37	5.71

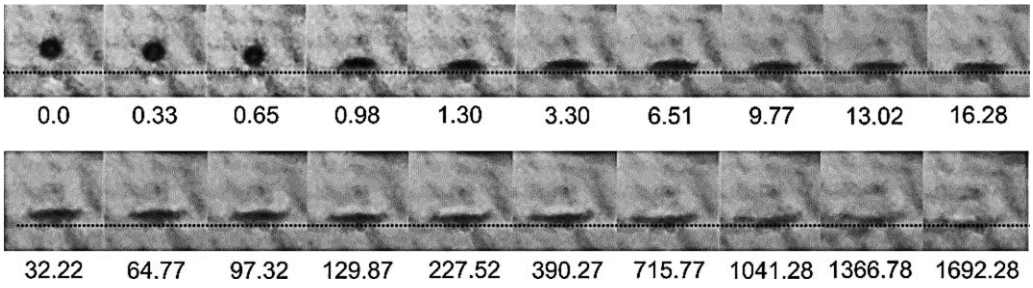

Figure 4. Sequence of images for drop deposition and solvent evaporation with a time scale in ms; the observation angle of camera was set at around 10° from the horizontal substrate.

accessory was employed. A series of PAA/NMP inks were cast and dried at 100 °C, these samples were then heat treated at different temperatures (140 °C, 160 °C, 180 °C, and 200 °C) for up to 60 min. A reference PI film with a theoretical 100% conversion rate was prepared by subsequently heating the PAA films in air at 200 °C and 250 °C for 0.5 h and 350 °C for 1 h.[4]

Inkjet Deposition Assessment

Following printability assessment, the PAA/NMP inks were printed using a Dimatix DMP 2830 printer (Fujifilm). The prepared 1 wt %, 3 wt %, and 5 wt % inks were filtrated (HPLC Nylon 5.0 μm syringe filters, Cole-Parmer) and injected into the print cartridge (DMC-11610, 10 pl), which was fixed to a printhead consisting of 16 nozzles (21 μm in diameter). After obtaining a stable droplet by setting cartridge temperature to 30 °C, using a dual-peak printing waveform and printing voltages between 20 V and 28 V, different patterns (individual droplets, lines, and films) were printed on glass substrates (microscope slides, Cole-Parmer) to study the printing quality. The microscope slides were sonicated with isopropanol before using. Patterns were printed using different droplet velocities (6 m s^{-1}, 8 m s^{-1}, 10 m s^{-1}) and droplet spacings (20 μm, 30 μm, 40 μm, 60 μm). The glass substrates were heated and held at different temperatures (100 °C, 140 °C, 160 °C) during the printing process to enable the solvent evaporation and thermal imidization.

Droplet Formation Process

The droplet formation process was continuously recorded using a high speed camera (Photron APX RS Fastcam) at 3000 frame per second (fps) and a shutter speed of 1/40,000 s. The droplets were deposited onto a glass substrate using either a Dimatix cartridge or a syringe, and the glass substrate was heated to 160 °C and 140 °C, respectively, with a thin film heater (KHLV-103/5 Kapton insulated flexible heater, Omega).

Morphology of Printed PI Films

A Nikon Reichert-Jung MEF3 optical microscope was used to characterise the dot sizes, bead widths as well as the general surface morphology of printed samples. Detailed surface morphology of the printed samples was characterised using a Fogale Photomap 3D Interferometer.

Dielectric Properties of PI Films

A series of parallel plate capacitors were printed to determine the dielectric properties of the printed PI thin films as illustrated in Figure 2(a). Two, three, and four layers of PI squares (size 7 mm × 7 mm) were printed on to Aluminum substrates, followed by three layers of silver nanoparticle ink (Advanced Nano Products Co. Ltd) printed (5 mm × 5 mm) on top of the PI. Apart from using a normal pattern in Figure 2(b), a pattern with 30% overlap between each line was also employed to reduce any surface undulations and defects of the PI film surface, as illustrated in Figure 2(c).

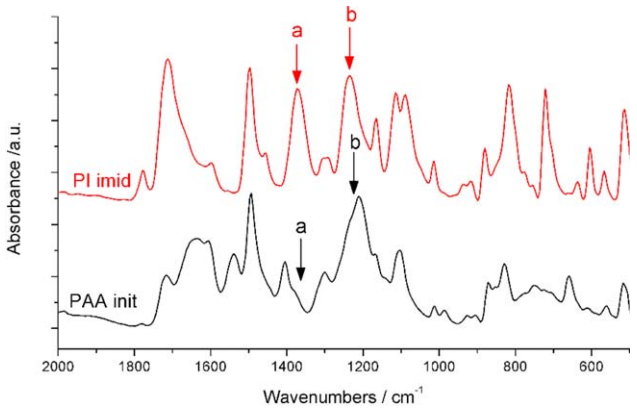

Figure 5. IR spectra of PAA film before (PAA init) and after (PI imid) the thermal imidization process. Two peaks, marked a and b, were identified at around 1375 cm^{-1} (C-N stretch of the imide group) and at 1235 cm^{-1} (C-O stretch of phenyl ether), and used to ascertain the degree of conversion to PI. [Color figure can be viewed in the online issue, which is available at wileyonlinelibrary.com.]

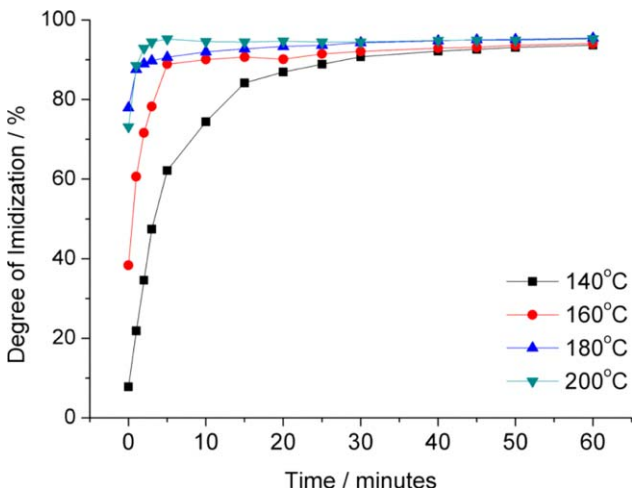

Figure 6. Effect of heating duration on the imidization degrees of PAA/NMP solutions heated at 140 °C, 160 °C, 180 °C, and 200 °C. [Color figure can be viewed in the online issue, which is available at wileyonlinelibrary.com.]

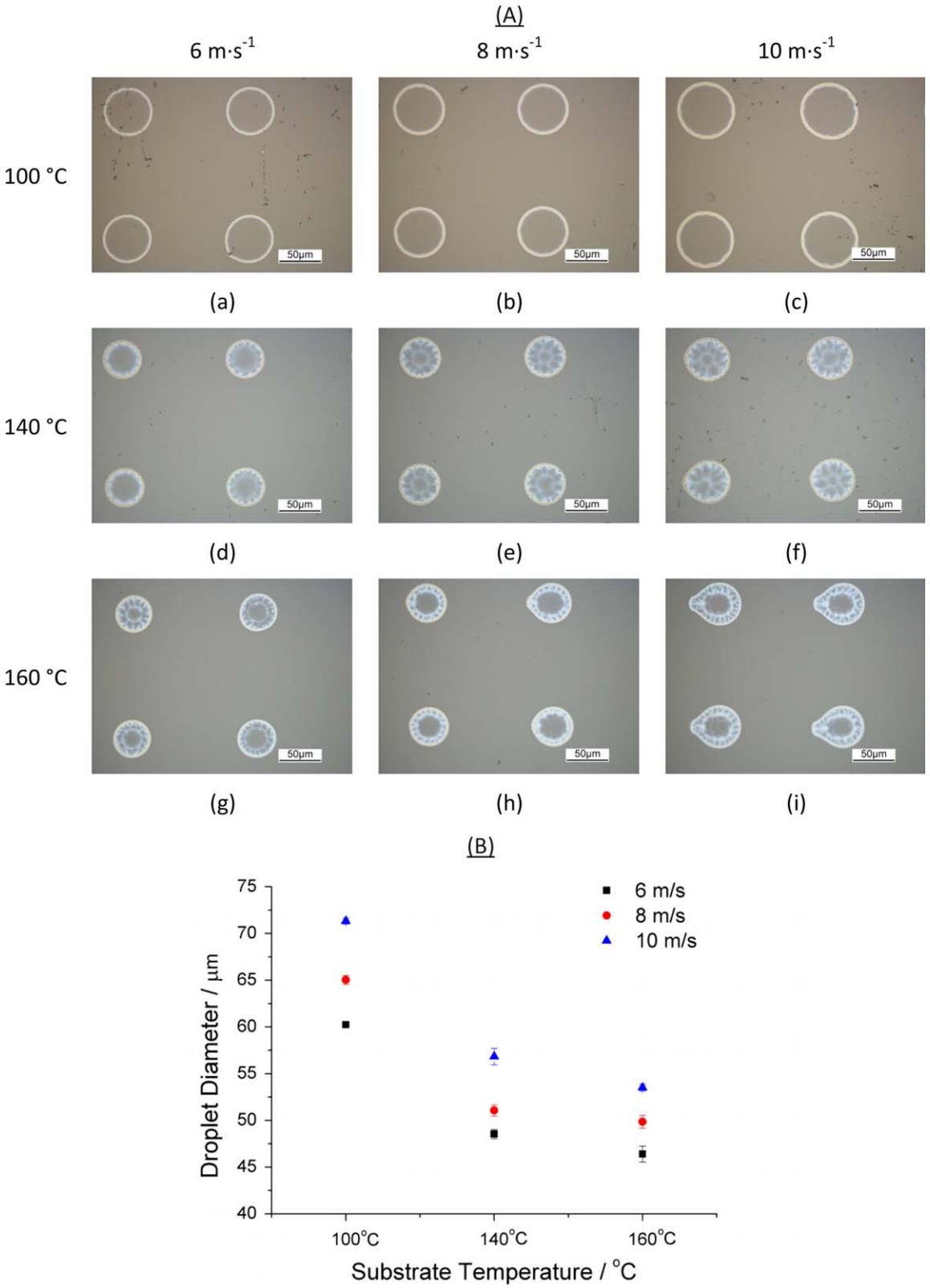

Figure 7. (a) Optical microscopy result of deposited and solidified PAA/PI printed with different droplet velocities and substrate temperatures. (b) Effects of droplet velocity and substrate temperatures on the droplet diameter. [Color figure can be viewed in the online issue, which is available at wileyonlinelibrary.com.]

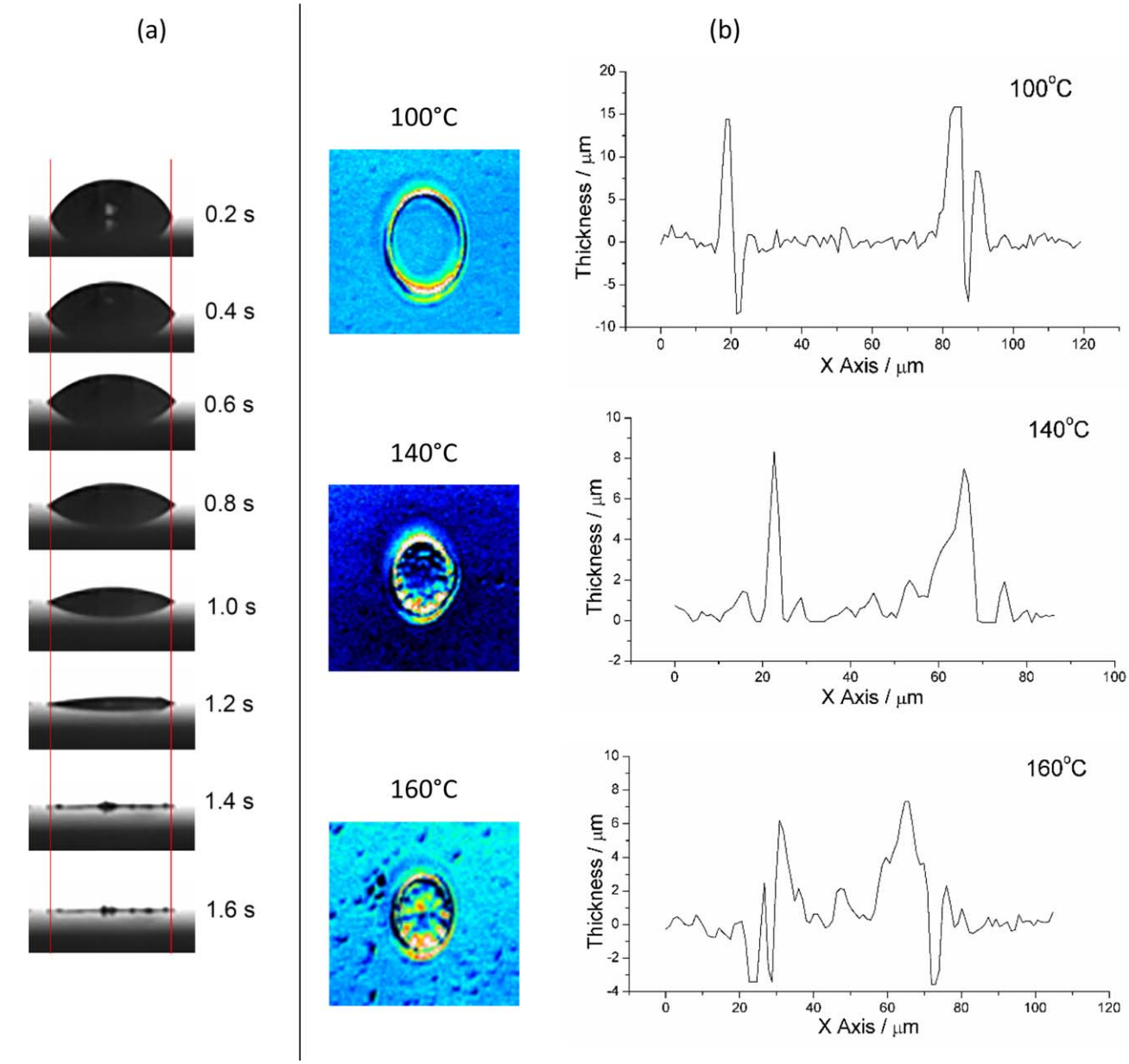

Figure 8. (a) Solvent evaporation process of a deposited droplet on glass substrate at 140 °C and (b) surface profiling results of droplets deposited on glass substrates at 100 °C, 140 °C and 160 °C. [Color figure can be viewed in the online issue, which is available at wileyonlinelibrary.com.]

A reference capacitor (10 mm × 10 mm) with a 25-μm thick PI layer was printed to calculate the dielectric constant of the printed PI polymer. All the capacitance values were measured using a LCR meter (R&S HM8018) at 1 kHz.

RESULTS AND DISCUSSION

Ink Printability

As can be seen from the results shown in Figure 3, the viscosity of PAA/NMP inks increased with increasing PAA content, but reduced with increasing temperature. The viscosity ranges for 1 wt %, 3 wt %, and 5 wt % solutions were found to be within 0.001 to 0.005 Pa s, 0.005 to 0.018 Pa s, and 0.014 to 0.040 Pa s, respectively. The initial test results showed that 5 wt % ink was not printable even at 70 °C, which may have been due to solvent evaporation leading to PAA precipitating around the nozzle and causing clogging. For 3 wt % ink, stable droplets were achieved at temperatures above 50 °C. However, it was found that in later tests that at such high temperatures the print head could be damaged by the strong organic solvent NMP. As a result the 1 wt % ink was chosen due to it having the lowest viscosity being printable at 20 °C. This ink formed stable droplets without obvious damage to the print head.

After measuring the density and surface tension of the 1 wt % ink at 20 °C, the printability index Z number was calculated to be 5.71, as shown in Table I. This ink was subsequently demonstrated to be printable.

Droplet Formation Process

As a solvent based ink, the droplet formation process of PAA/NMP ink can be further divided into three sub-steps: droplet pinning, solvent evaporation, and the thermal imidization.[4] Due to the

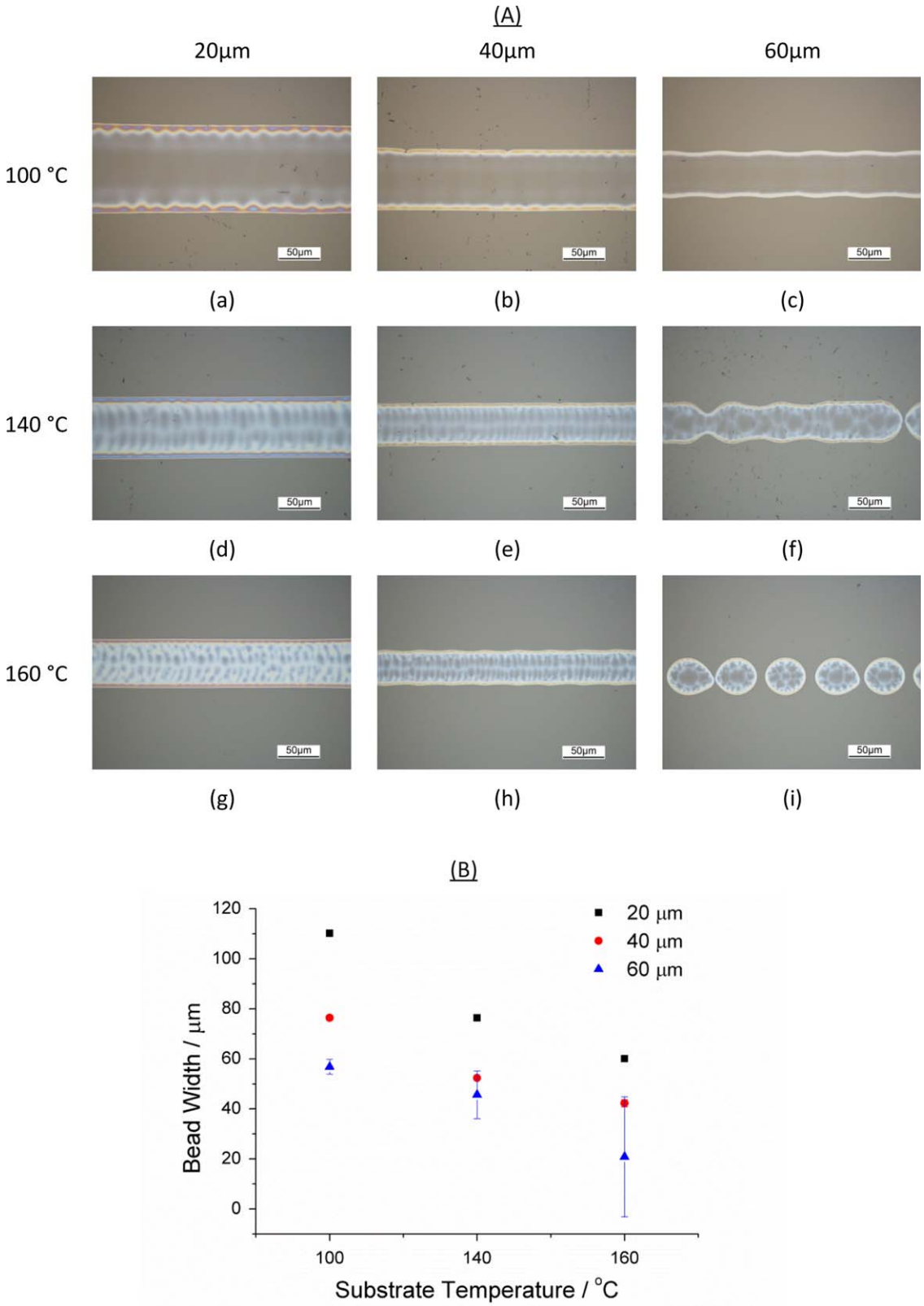

Figure 9. (a) Optical microscopy result of line formation for PAA/PI printed with different droplet spacings and substrate temperatures. (b) Effects of droplet spacing and substrate temperature on the bead widths. [Color figure can be viewed in the online issue, which is available at wileyonlinelibrary.com.]

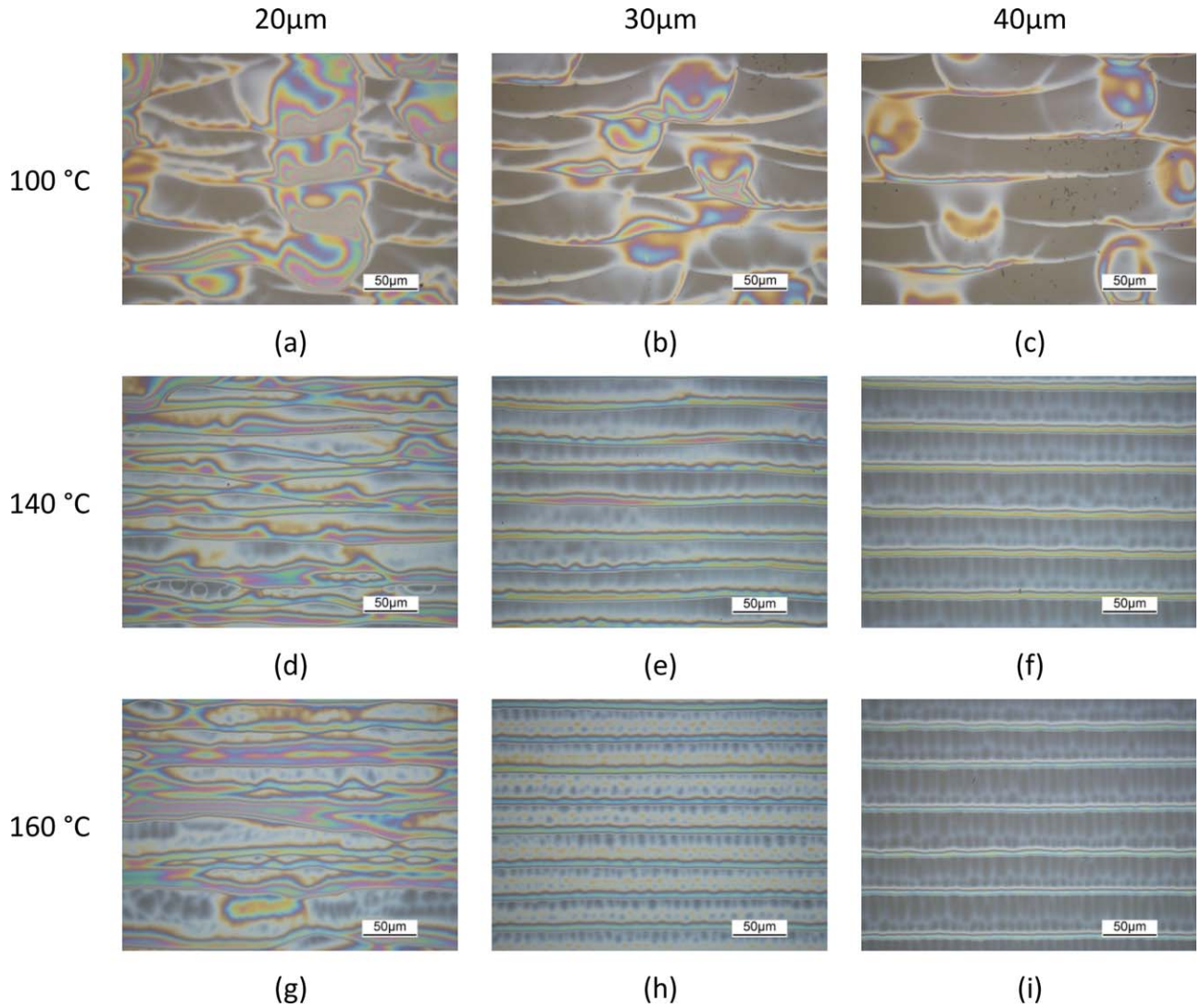

Figure 10. Optical microscopy result of printed PAA/PI films with different droplet spacings and substrate temperatures. [Color figure can be viewed in the online issue, which is available at wileyonlinelibrary.com.]

limitation of the experimental apparatus, the detailed droplet impaction process could not be observed. However, the approximate time scale for each sub-step can be observed from Figure 4.

It can be reasoned from Figure 4 that the droplet impacted and fixed to the substrate within 16 ms, which is similar to the results reported by Dong *et al.*[15] The solvent evaporation took much longer time than droplet pinning, which was approximately 1400 ms. Solvent evaporation is a physical process that fixes the solid component following deposition, while thermal imidization is the chemical process during which PAA loses water molecules to form PI. These two subprocesses may take place simultaneously, and any remaining solvent can act as an effective plasticizer for the imidization.[4] The thermal imidization subprocess requires much longer time to reach a reasonable high conversion rate, which will be discussed in the next section.

Thermal Imidization Process

Figure 5 shows the IR spectra of PAA film dried at 100 °C (PAA init) and the reference PI film (PI imid). A sharp peak at around 1375 cm^{-1} (peak a) assignable as a C-N stretch of the imide group was observed in PI but not in PAA, indicating the formation of PI. The peak at 1235 cm^{-1} (peak b), which was assigned to the C-O stretch of phenyl ether, was selected as the reference peak, as this structure would remain the same before and after the reaction, and would not be influenced by the solvent.[4] By comparing the intensities of these two peaks, the degree of imidization was determined using the following equation.[4,16,17]

$$\text{Degree of imidization } (\%) = \frac{\text{a/b[sample]} - \text{a/b [init]}}{\text{a/b[imid]} - \text{a/b[init]}} \times 100\% \quad (2)$$

where [sample] stands for the PAA films heat treated at different conditions; [init] is the PAA ink dried at 100 °C without imidization; [imid] is the reference PI film which is fully cured at 350 °C for 1 h.

Figure 6 shows the effects of heating temperature and duration on the degree of imidization of PI films. As the temperature increased from 140 °C to 200 °C, the time required for maximum degree of

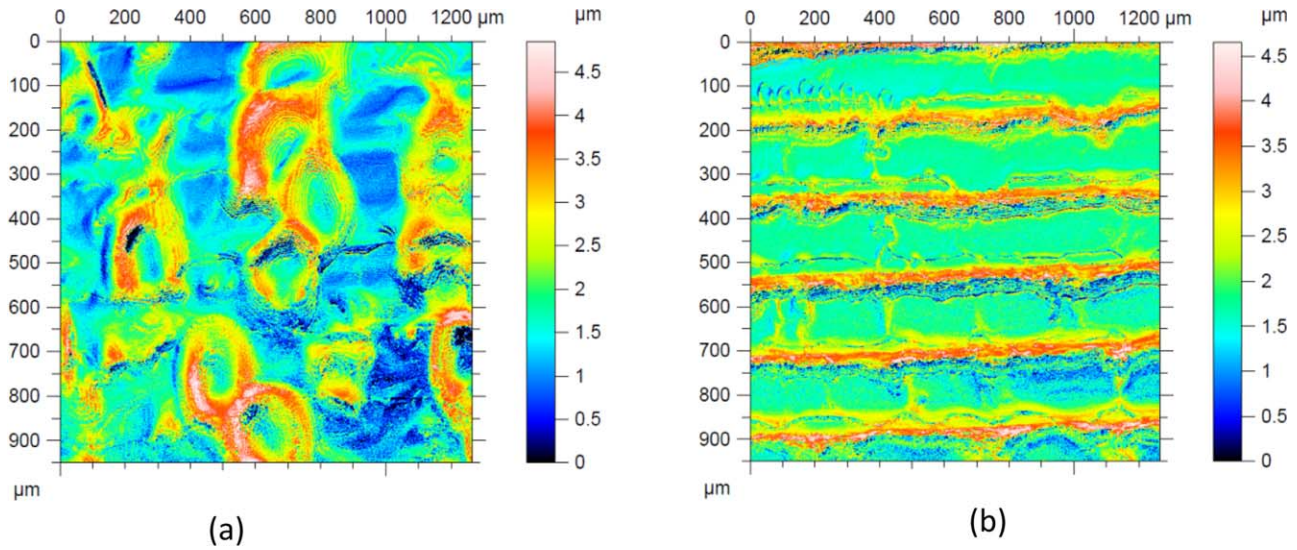

Figure 11. Surface profiling results of (a) bulges on film printed at 100 °C with 30 μm droplet spacing and (b) regular waviness on film printed at 160 °C with 30 μm droplet spacing. [Color figure can be viewed in the online issue, which is available at wileyonlinelibrary.com.]

imidization reduced from 40 min to 3 min. The maximum degree of imidization showed little change with different heating temperatures. For samples heated at and above 180 °C, the degree of imidization was seen to be close to 100% within 10 min. These results suggested the possibility of continuously printing PI films by printing directly on to higher temperature substrates, which will be introduced in the following sections.

Droplet Deposition

The substrate temperature is a key variable since solidification of PAA inks is based on a solvent evaporation process. The effects of substrate temperature and droplet velocity on the deposited ink droplet were observed using optical microscopy as shown in Figure 7(a), and their corresponding droplet sizes were measured [Figure 7(b)]. Three substrate temperatures, 100 °C, 140 °C, and 160 °C, were chosen. At 100 °C, the NMP solvent of the PI ink evaporates slowly, allowing the ink to flow before curing. At 140 °C, the ink cures much faster than at 100 °C. 160 °C is the temperature for full imidization, which allows PI to be directly printed without the need for post thermal treatment.

It was observed from Figure 7(b) that the droplet sizes reduced with decreasing droplet velocity and increasing temperature. A higher droplet velocity caused a stronger impact during the printing process, making the ink spread to a larger area.[15] According to the results, both 6 m s^{-1} and 8 m s^{-1} of droplet velocities showed a good consistency of droplet formation, which are selected for printing.

The solvent evaporation process of a deposited droplet on glass substrate at 140 °C was recorded with a high speed camera as shown in Figure 8(a), it can be seen from which that the ink tended to move outward during this process, resulting in larger droplet sizes.[15] Higher temperatures increased the evaporation rate of the solvent, leaving the ink less time to spread and resulting in a reduced observed deposition diameter. The surface profiling results of the deposited droplets are shown in Figure 8(b), from which ring-like deposits are observed in all dried droplets due to Coffee ring effects.[18,19] The widths of ring walls became thicker as the substrate temperature increased from 100 °C to 160 °C, likely leading to a reduction in the deposition diameter while the solid content remained unchanged.

Line Formation

Droplet spacing, which is the distance between adjacent droplets, is an important factor that determines the quality of the printed lines or films. The degree of droplet spacing is normally determined by the value of the droplet diameter. In order to study the effects of the droplet spacing, lines with various droplet spacing values were printed at different substrate temperatures, and three droplet spacing values, 20 μm, 40 μm, and 60 μm, were chosen, with the droplet velocity set at 8 m s^{-1}, as shown in Figure 9(a,b).

Firstly, it was first found that the bead width decreased with increasing substrate temperature, which was due to the reduction of droplet diameter at higher temperatures, as discussed in the Ink Printability section. Secondly, it was also observed that increased droplet spacing caused a decreased bead width. This is because a low droplet spacing (i.e., 20 μm) may cause overlapping of the droplets, resulting in a large volume of ink within the area.[20] If the volume of the ink within the area was too large and the contact angle was larger than the advancing angle, the ink would tend to move outwards, increasing the bead width.[20] A high droplet spacing (i.e. 60 μm) would result in narrow or even discontinuous lines, as there was not enough ink to fill the whole printing area. Therefore, a suitable droplet spacing is essential for the good results. As can be seen from Figure 9(a), continuous lines were obtained using both 20 μm and 40 μm droplet spacings.

Film Formation

For film formation, the droplet spacing not only determines the quality of separate lines as discussed in the Droplet Formation Process section, but also affects the interfaces between these lines. In this section, films with three different droplet spacings, 20 μm, 30 μm, and 40 μm, were printed at various temperatures, with their optical microscopy images shown in Figure 10.

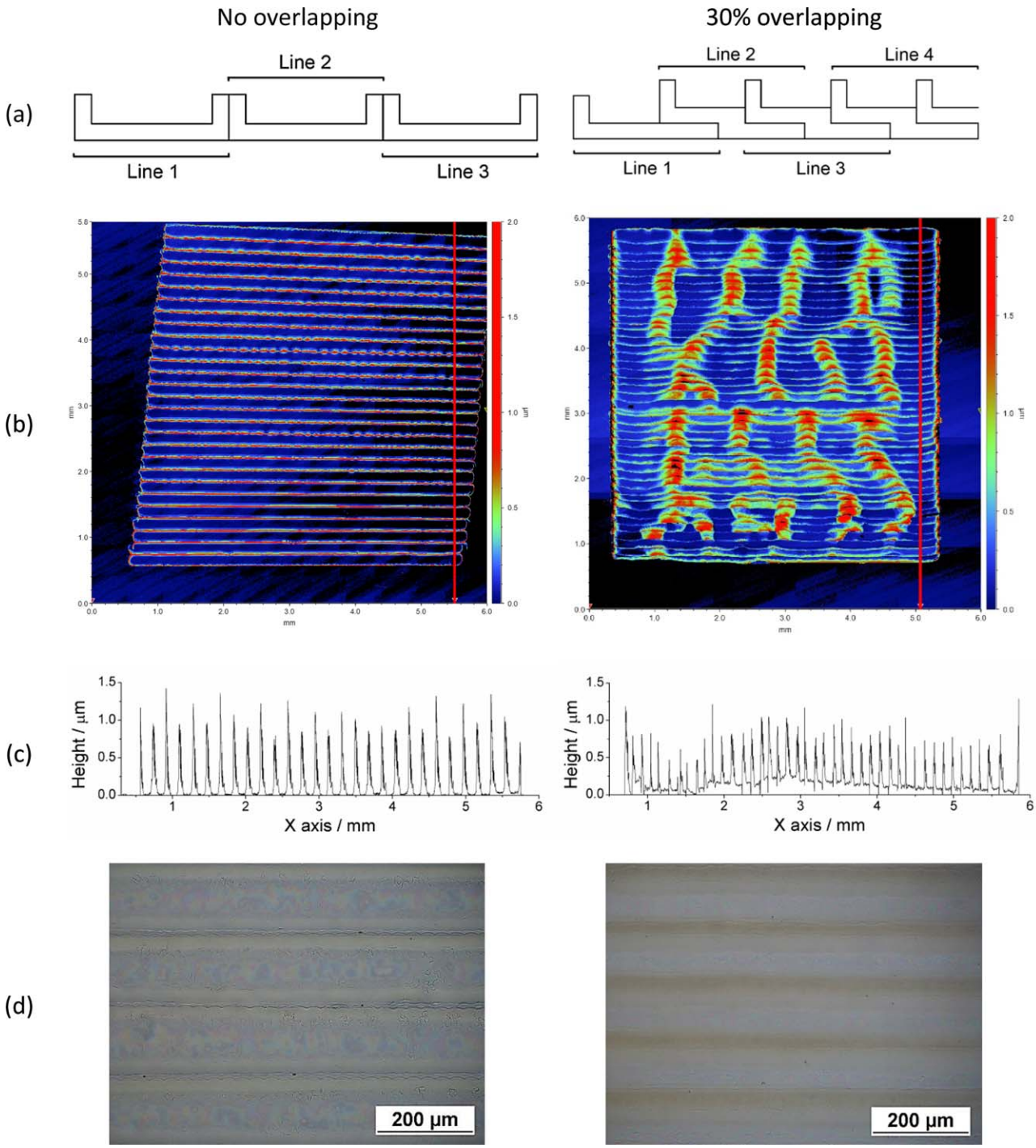

Figure 12. (a) Pattern with no overlapping (left) and pattern with 30% overlapping between each line (right); (b) two-dimensional surface profile results; and (c) their corresponding one-dimensional profile results across the marked positions of the printed PI films with no overlapping (left) and 30% overlapping (right); and (d) optical microscopy images of printed films with no overlapping (left) and 30% overlapping (right). [Color figure can be viewed in the online issue, which is available at wileyonlinelibrary.com.]

As can be seen from the results, crater-like formations were observed in all films printed at 100 °C (a–c), which was probably due to the slow solvent evaporation and too small droplet spacing. According to Gao and Sonin, who reported similar phenomenon during the printing of wax, a too small droplet spacing would cause the ink to become unstable and begin to swell.[21] For films printed with droplet spacings of 20 μm and 40 μm, the bead widths at 100 °C were measured to be around 110 μm and 76 μm, respectively, which were much larger than the droplet spacing values. At this temperature, the printed droplet tended to merge with previously unsolidified ink due to the relatively slow solvent evaporation, causing a large volume of ink within the area, as illustrated in Figure 11(a). During the curing process, this large volume of ink tended to swell to reduce the surface tension,[20,21] leaving crater-like formations on the film surface.

Table II. R_a and R_z Measures of the Non-Overlapping Film, the Consistent Printing Regions of the 30% Overlapping Film and the "Build-Up" Regions of the Overlapping Film

	Non-overlapping film	30% Overlapping film – consistent printing areas	30% Overlapping film – areas of 'build-up'
R_a (μm)	0.19 ± 0.019	0.19 ± 0.016	1.1 ± 0.14
R_z (μm)	3.2 ± 0.70	1.9 ± 0.15	2.5 ± 0.59

As shown in Figure 11(b), crater-like formations disappeared when substrate temperatures reached 140 °C and 160 °C, as at such temperatures, the droplet solidified before the next row of ink was jetted. However, in this case, a boundary interface between two rows appeared, resulting in periodic ridges in all of these films. As the substrate temperature increased, the printed ink droplet evaporated more rapidly, leaving the solvent less time to dissolve the solidified thread, making the periodic ridge pattern more regular.[22] These ridges may not be significant for a film with only one layer, however, as the number of layers increases, the periodic ridges could build up and significantly reduce the insulating properties of the PI films.

Effect of Overlapping

Due to the periodic ridges shown on the film surface, some parts of the film were thinner than others, which reduced the insulating properties of the whole film. Therefore, a 30% overlapping between each line was employed to reduce the ridge effects and defects of the film surface, as illustrated in Figure 12.

Because of the Coffee ring effects and the fact that separated adjacent drops were printed with smaller separations, periodic ridges were formed at the edges of lines instead of crater-like formations.[18,19,23] As illustrated in Figure 12(a) (left), these ridges could build up during the printing process, causing negative effects to the insulating properties of the films. By introducing 30% overlapping into the pattern [Figure 12(a); right], these ridges could be reduced by being distributed across the whole film. As can be observed from Figure 12(b–d), films with overlapping patterns showed reduced distance between ridges, meaning there was a higher density of printed lines in the Y direction. Surface profiling of PI films with and without overlap shows that the difference between "ridges" and "valleys" can be reduced. For example, for printing three layers without overlap the height of the ridges was 1.040 ± 0.196 μm, with a valley height of 0.016 ± 0.009 μm. By introducing 30% overlapping into the films, the height of the ridges decreased to 0.827 ± 0.193 μm, while the valley increased to 0.130 ± 0.059 μm, demonstrating the possible reduction in range of heights when overlapping. This potential for building up the layer in a more consistent manner does come with some disadvantages however, as more complex topologies may emerge [Figure 12(b)]. Results of a surface analysis of the two types of morphologies are shown in Table I. For the overlapping film, measurements were made on regions of "build-up" and regions of consistent line printing, to avoid any systematic errors. As a result, Table I shows a comparison of the average surface height, R_a, and average range between peaks and valleys, R_z, for nonoverlapping, overlapping regions with consistent line printing and overlapping regions with "build-up." This shows that away from the build-up zones, overlapping does not affect R_a strongly, but does reduce R_z significantly. In regions where there is build up, the height is increased, but the roughness is again smoothed. This approach suggests that by tuning and optimizing the overlap, a more consistent surface can be achieved and future efforts will need to focus on reducing the potential for localized build up to occur and propagate in the film Table II.

DIELECTRIC PROPERTY OF PRINTED PI FILMS

Effects of Overlapping on the Insulating Property

To test the dielectric properties, the PI ink was printed onto aluminum substrates instead of glass in order to incorporate one of the electrodes as the substrate. The contact angles of the PI ink on aluminum and glass substrates were found to be 9.6° ± 1.4° and 7.0° ± 0.6°, respectively, suggesting that similar morphologies on these substrates would be obtained.

Dielectric Constant of the Printed PI Film

A capacitor (10 mm × 10 mm) with a 25 ± 0.2 μm thick PI layer was printed as a reference sample to calculate the dielectric constant of the PI polymer [Figure 2(a)]. The capacitance value at 1 kHz was evaluated to be around 103 pF, which led to a relative permittivity of 2.90 ± 0.02.

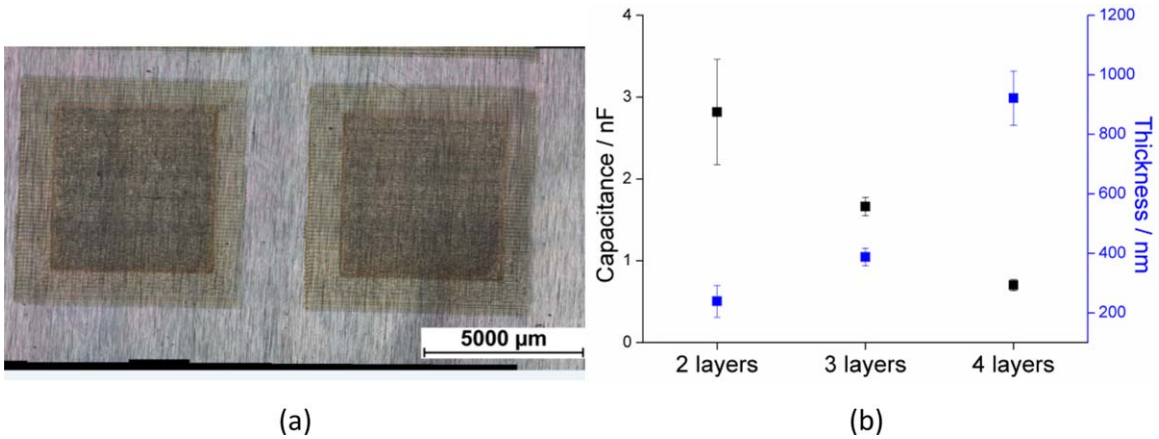

Figure 13. (a) Parallel plate capacitors fabricated using inkjet printing; (b) capacitance values and corresponding PI equivalent thicknesses of the printed capacitors. [Color figure can be viewed in the online issue, which is available at wileyonlinelibrary.com.]

$$\varepsilon_r = \frac{Cd}{\varepsilon_0 A} \quad (3)$$

$$\varepsilon_r = \frac{Cd}{\varepsilon_0 A} = \frac{103 \times (0.000025 \pm 0.0000002)}{8.85 \times 10^{-12} \times 0.0001} = 2.90 \pm 0.02$$

where C is the capacitance, d is the thickness, A is the area, and ε_0 is the dielectric constant of free space. This compares well with reference results that lie in the range between 2.8 and 3.2.[24] Therefore, a dielectric constant of 2.90 was used for the following experiments.

Thin Film Capacitors

A series of capacitors with various PI thicknesses (two, three, and four layers of PI) were printed as shown in Figure 13(a). For each thickness, 24 samples were prepared and tested, with their capacitance results at 1 kHz frequency shown in Figure 10(b). Using these results, the "equivalent thicknesses" of the PI layers were calculated. Equivalent thickness is an indication of the quality of the PI layer. The capacitance value reduced with increasing layer number, and the highest capacitance was achieved by two layers of PI, which was 2.82 ± 0.64 nF. These results showed that inkjet printing method can be used to fabricate PI insulating layer thinner than 1 μm, suggesting wide applications in many electronic devices such as diode, transistor, etc.

CONCLUSIONS

In this article, PI insulating layers were successfully prepared using inkjet printing method from its precursor PAA. FT-IR results showed that PAA could convert to PI by heating above 160 °C for more than 15 min, making it possible to print PI samples continuously. The printability of PAA ink was systematically studied, with the effects of droplet velocity, substrate temperature, and droplet spacing on the surface morphology of the samples carefully compared and examined. It was observed that as the substrate temperature increased, the film surface tended to show regular waviness rather than random bulges, and this predictable waviness was compensated by introducing 30% overlapping between lines. The insulting property of the printed PI layer was examined by sandwiching it between two conducting layers, and 24 parallel samples were prepared for each setting to confirm the repeatability of the results. The thinnest PI insulating layer was achieved by two layers of PI, which showed a capacitance value of 2.82 ± 0.64 nF, with an equivalent thickness below 1μm. The results of this work showed the possibility of preparing PI insulating layer using inkjet method. This new continuous PI printing process potentially provides a more versatile and efficient way for the fabrication of microelectronic devices compared with the traditional methods.

ACKNOWLEDGMENTS

The authors would like to acknowledge funding support from University of Nottingham, the EPSRC (Grant number EP/I033335/2).

REFERENCES

1. Lai, J. H.; Douglas, R. B.; Donohoe, K. *Ind. Eng. Chem. Prod. Res. Dev.* **1986**, *25*, 38.
2. Ogura, T.; Higashihara, T.; Ueda, M. *J. Polym. Sci. Part A: Polym. Chem.* **2009**, *47*, 3362.
3. Diaham, S.; Locatelli, M.-L.; Khazaka, R. BPDA-PDA Polyimide: Synthesis, Characterizations, Aging and Semiconductor Device Passivation, High Performance Polymers - Polyimides Based - From Chemistry to Applications, Abadie M.; Ed., ISBN: 978-953-51-0899-3, InTech, **2012**. DOI: 10.5772/53994. Available at: http://www.intechopen.com/books/high-performance-polymers-polyimides-based-from-chemistry-to-applications/bpda-pda-polyimide-synthesis-characterizations-aging-and-semiconductor-device-passivation.
4. Fukukawa, K.; Shibasaki, Y.; Ueda, M. *Chem. Lett.* **2004**, *33*, 1156.
5. Zhang, M. C.; Kang, E. T.; Neoh, K. G.; Cui, C. Q.; Lim, T. B. *Polymer (Guildf).* **2001**, *42*, 453.
6. Wilson, W. C., Atkinson, G. M. Review of Polyimides Used in the Manufacturing of Micro Systems; Technical Report, NASA Langley Research Center, Hampton, VA, United States, Report Number: NASA/TM-2007-214870, L-19339, **2007**, http://ntrs.nasa.gov/search.jsp?R=20070018345.
7. Liu, Y.; Cui, T.; Varahramyan, K. *Solid State Electron.* **2003**, *47*, 1543.
8. Jensen, G. C.; Krause, C. E.; Sotzing, G. A.; Rusling, J. F. *Phys. Chem. Chem. Phys.* **2011**, *13*, 4888.
9. ASTM. F2792 standard terminology for additive manufacturing technology, **2012**. Available at: http://www.astm.org (accessed 15 December 2015)
10. Yang, Y.; Naarani, V. *Dye Pigment* **2006**, *74*, 154.
11. Sun, Y. Y.; Zhang, Y. J.; Liang, Q.; Zhang, Y.; Chi, H. J.; Shi, Y.; Fang, D. N. *RSC Adv.* **2013**, *3*, 11925.
12. Walker, S. B.; Lewis, J. *J. Am. Chem. Soc.* **2012**, *134*, 1419.
13. Ainsley, C.; Reis, N.; Derby, B. *J. Mater. Sci.* **2002**, *37*, 3155.
14. Jang, D.; Kim, D.; Moon, J. *Langmuir* **2009**, *25*, 2629.
15. Dong, H.; Carr, W. W.; Morris, J. F. *Rev. Sci. Instrum.* **2006**, *77*.
16. Diaham, S.; Locatelli, M. L.; Lebey, T.; Malec, D. *Thin Solid Films* **2011**, *519*, 1851.
17. Ahn, T.; Choi, Y.; Jung, H. M.; Yi, M. *Org. Electron. Phys. Mater. Appl.* **2009**, *10*, 12.
18. Deegan, R. D.; Bakajin, O.; Dupont, T. F.; Huber, G.; Nagel, S. R.; Witten, T. A. *Phys. Rev. E: Stat. Phys. Plasmas Fluids Relat. Interdiscip. Top.* **2000**, *62*, 756.
19. Deegan, R. D. et al. *Nature* **1997**, *389*, 827.
20. Thompson, A. B.; Tipton, C. R.; Juel, A.; Hazel, A. L.; Dowling, M. *J. Fluid Mech.* **2014**, *761*, 261.
21. Gao, F.; Sonin, A. A. *Proc. R. Soc. Lond. A Math. Phys. Eng. Sci.* **1994**, *444*, 533.
22. Lee, J. K.; Lee, U. J.; Kim, M. K.; Lee, S. H.; Kang, K. T. *Thin Solid Films* **2011**, *519*, 5649.
23. Stringer, J.; Derby, B. *Langmuir* **2010**, *26*, 10365.
24. Ahmad, Z. Polymer Dielectric Materials, Dielectric Material, Alexandru Silaghi M.; Ed., ISBN: 978-953-51-0764-4, InTech, **2012**. DOI: 10.5772/50638. Available at: http://www.intechopen.com/books/dielectric-material/polymer-dielectric-materials.